

The role of advection in the accreting corona model for active galactic nuclei and Galactic black holes

A. Janiuk¹, P.T. Życki^{2,1}, B. Czerny¹

¹*N. Copernicus Astronomical Center, Bartycka 18, 00-716 Warsaw, Poland*

²*Department of Physics, University of Durham, Durham DH1 3LE*

5 March 2022

ABSTRACT

We consider the role of advection in the two-temperature accreting corona with an underlying optically thick disc. The properties of coronal solutions depend significantly on the description of advection. Local parameterization of advection by a constant coefficient δ replacing the radial derivatives lead to complex topology of solutions, similar to some extent to other advection-dominated accretion flow solutions. One, radiatively cooled branch exists for low accretion rates. For higher accretion rates two solutions exist in a broad range of radii: one is radiatively cooled and the other one is advection-dominated. With further increase of accretion rate the radial extensions of the two solutions shrink and no solutions are found above certain critical value. However, these trends change if the local parameterization of advection is replaced by proper radial derivatives computed iteratively from the model. Only one, radiatively cooled solution remains, and it exists even for high accretion rates. The advection-dominated branch disappears during the iteration process which means that a self-consistently described advection-dominated flow cannot exist in the presence of an underlying cold disc.

Key words: galaxies: active – accretion, accretion discs – black hole physics – binaries – X-rays; stars – galaxies:Seyfert, quasars – X-rays.

1 INTRODUCTION

There are direct observational evidences that the gas surrounding central black holes in active galactic nuclei (AGN) and in galactic black holes (GBH) consists of two phases: colder, optically thick phase and hotter optically thin phase (for a review, see Mushotzky, Done & Pounds 1993; Tanaka & Lewin 1995; Madejski 1999). The emission of radiation is clearly powered by accretion onto the black hole. However, it is still not clear which of the two phases is responsible for accretion.

In the classical disc/corona models (e.g. Liang & Price 1977; Bisnovaty-Kogan & Blinnikov 1977; Haardt & Maraschi 1991) the accretion proceeds through the disc and the coronal gas does not contribute significantly to the angular momentum transfer, presumably because of its magnetic coupling to the disc.

In clumpy accretion flow models the accretion proceeds predominantly through the cold clumps of gas (Collin-Souffrin et al. 1996, Czerny & Dumont 1998; Krolik 1998; see also Torricelli-Ciamponi & Courvoisier 1998).

However, there are also models in which the hot gas carries most of the mass. The division of the flow into the two

phases is predominantly radial in models based on advection dominated accretion flow (ADAF) solutions (e.g. Ichimaru 1977; Abramowicz et al. 1995; Narayan, Kato & Honma 1997; Esin, McClintock & Narayan 1997), in the Compton cooled solutions for ion tori (Shapiro, Lightman & Eardley 1976; hereafter SLE), or in models considering both cooling mechanism (Björnsson et al. 1996). In those models the accretion proceeds through the cold accretion disc in the outer region and through the hot plasma region in the inner region.

In this paper we discuss the model of an accreting corona. Initial formulation of the basic assumptions was given by Życki, Collin-Souffrin & Czerny (1995) and the final formulation of the model was outlined by Witt, Czerny & Życki (1997; hereafter WCZ). In this model the accretion proceeds both through a disc and a corona, in proportions determined by the model and varying with the distance from the black hole. The model was applied to Nova Muscae 1991 (Czerny, Witt & Życki 1996) and AGN (Czerny, Witt & Życki 1997).

In this paper we address the problem of advection in the corona. An optically thin accreting corona should show similar general behavior as a general optically thin flow not

accompanied by the disc, i.e. we might expect both advection dominated solutions and radiatively cooled solutions. Advection was included in the model by WCZ and was found to be always negligible. Here we explain the nature of this phenomenon.

2 MODEL

2.1 Corona structure

We assume that the corona itself accretes, i.e. that the energy in the corona is due to the direct release of the gravitational energy in the hot phase, without the necessity of having a mediator (e.g. magnetic field) between the disc and the corona. We further assume that the energy release can be described by the α viscosity prescription of Shakura & Sunyaev (1973), with the energy generation rate proportional to the gas pressure (we neglect radiation pressure in the corona because the corona is optically thin).

We assume a two-temperature plasma in the corona as in the classical paper of SLE, i.e. the ion temperature is different from the electron temperature. The energy balance is computed assuming that the release of gravitational energy heats the ions, the Coulomb coupling transfers this energy to electrons and finally electrons cool down by inverse Compton process, with the disc emission acting as a source of soft radiation flux. The hot corona is radiatively coupled to the disc, as described by Haardt & Maraschi (1991). We assume isotropic emission within the corona ($\eta = 1/2$) and for the (energy integrated) disc albedo we adopt a value $a = 0.2$. Compared to our previous paper (WCZ) we now use an accurate prescription for the Compton amplification factor, A (defined by $F_c = A F_{\text{soft}}$), namely we compute A from Monte Carlo simulations of Comptonization. Our Monte Carlo code employs the method described by Pozdnyakov, Sobol & Sunyaev (1983) and Górecki & Wilczewski (1984). Assuming slab geometry (Thomson optical depth τ_{es} and electron temperature T_e) and the soft photons spectrum as a black body of temperature T_s , we compute A on a grid of T_e , τ_{es} , and T_s and interpolate for values of interest at each radius.

We neglect the dynamical term in the corona since it was shown to be relatively unimportant (WCZ). Therefore we can assume that the corona is in hydrostatic equilibrium and instead of solving original complex differential equations we adopt a set of simplified equations given in Appendix D of WCZ, with modifications concerning the advection and the Compton amplification factor. We also neglect the effect of the vertical outflow of the gas from the corona discussed by WCZ, i.e. we assume that the total accretion rate (the sum of accretion rates through the disc and the corona) is constant, independent of radius.

2.2 Disc–corona transition

The main feature of the model is that the division of the accretion flow into the hot and cold phases is not arbitrary. The thermal instability in an irradiated medium (Krolik, McKee & Tarter 1981) results in its spontaneous stratification into two stable phases. The criterion for the transition

from cold to hot phase is formulated in terms of a specific value of the ionization parameter Ξ which we define as

$$\Xi \equiv \frac{\eta F_c}{c P_{\text{gas}}} \quad (1)$$

where ηF_c is the fraction of the coronal flux directed towards the disc and P_{gas} is the coronal gas pressure (see also Krolik 1998). Following Begelman, McKee & Shields (1983) we adopt the following scaling,

$$\Xi = 0.65 (T_e / 10^8 \text{ K})^{-3/2} \quad (2)$$

where T_e is the electron temperature of the corona at a given radius.

This description of the disc/corona transition can be easily argued for in a qualitative way. The essence of the transition is a change from Compton cooling mechanism to atomic cooling, including bremsstrahlung. Therefore, the transition zone corresponds to certain assumed contribution of bremsstrahlung to the total cooling. The criterion (Eq. 2) applies accurately to the systems with either Compton heating of the corona or a heating proportional to the density and fixes the bremsstrahlung contribution to 2/3 of the total cooling. Similar criterion formulated by Krolik (1998) gives the value of 3/7. Since the relative bremsstrahlung contribution decreases rapidly with the departure from the transition zone into the corona, while the pressure remains roughly constant, we use this criterion as the basic criterion for pressure and we neglect bremsstrahlung as a cooling mechanism (see also Krolik 1998).

This additional equation enables us to actually determine the fraction of energy, f , which is liberated in the corona (N.B. in our previous paper WCZ we used $\xi \equiv 1 - f$). Since in our model f describes also the fraction of the mass accreting through the corona, we have

$$\dot{M}_c(r) = f(r)\dot{M}; \quad \dot{M}_d(r) = [1 - f(r)]\dot{M} \quad (3)$$

where \dot{M}_d , \dot{M}_c and \dot{M} are the disc, coronal and the total mass accretion rates. The total accretion rate does not depend on r if mass loss (e.g. through a wind as in WCZ) is neglected.

The formulation of the model allows for computing the corona structure independently from the disc internal structure. The disc/corona coupling is through surface pressure, P_{gas} , the coronal radiation flux, F_c and the disc soft flux, F_{soft} uniquely specified by f and albedo. There is no need for subsequent iterations between the computations of the corona structure and the disc vertical structure as long as the local disc emission is well approximated by a blackbody (more generally: a thermal emission with a constant ratio of the colour and effective temperatures) and the albedo is fixed. When the local corona parameters are determined, they provide the surface boundary conditions for the equations of the cold disc structure. The disc vertical structure can be solved if the viscous transfer within the disc is specified (Różańska et al. 1999). The imposed boundary conditions are automatically satisfied by the model, and the disc structure is determined uniquely.

The radial variation of the relative proportion of the disc and coronal accretion flows may mean that either a fraction of the coronal mass cools and settles down on the disc surface thus joining the disc flow instead of falling radially into black hole, or a fraction of the disc flow evaporates from

the disc surface and joins the coronal flow. These changes are forced by the requirement of the hydrostatic and thermal equilibrium between the disc and the corona at each radius. However, the dynamics of this phenomenon is beyond the scope of our present model.

2.3 Advection

In the present paper we include the advection term in the corona in all computations. The advection is described as in WCZ, i.e. the energy balance takes the form

$$F_c = F_{CC} + F_{adv} \quad (4)$$

and

$$4\pi r^2 F_{adv} = f(r) \dot{M} c_s^2 \delta; \quad \delta = \frac{d \ln P}{d \ln r} - \frac{5}{2} \frac{d \ln T_i}{d \ln r}, \quad (5)$$

where F_c is the energy flux generated in the corona, F_{CC} is the Compton cooling of the corona by the soft disc photons and c_s is the sound velocity in the corona. Equation 5 can be converted to give

$$\frac{F_{adv}}{F_c} = \delta \frac{T_i}{T_{vir}}, \quad (6)$$

where T_{vir} is the virial temperature,

$$T_{vir} \equiv \frac{GM}{r} \frac{m_H}{k}. \quad (7)$$

For the numerical solution of WCZ, $\delta = 0.75$ (see Appendix C in that paper). In general, however, δ is a function of radius and should be computed consistently. In the next Section we will show solutions for a number of fixed values of δ , while in Section 4 we will discuss solutions with δ determined consistently through iterations.

The parameters of the model are: the viscosity parameter α in the corona and the dimensionless accretion rate \dot{m} measured in the Eddington units

$$\dot{M}_{Edd} = 3.52 \frac{M}{10^8 M_\odot} [M_\odot / yr] \quad (8)$$

where M is the mass of the central black hole and we assumed the pseudo-Newtonian efficiency of accretion equal 1/16 and pure hydrogen opacities.

We show the results for the value of the viscosity parameter $\alpha = 0.3$ and the mass of the black hole $M = 10M_\odot$ but we discuss the trends of solutions with these parameters varied.

2.4 Spectra

At each radius, the equations of the structure of the corona determine the electron temperature, the optical depth of the corona and the soft photon flux from the disc. The effect of the Comptonization of the disc flux by the corona is calculated at each radius separately, using semi-analytical formulae of Czerny & Zbyszewska (1991). We neglect here the anisotropy of the Compton scattering which should be taken into account in detailed spectral modeling (e.g. Poutanen & Svensson 1996, Haardt, Maraschi & Ghisellini 1997). However, very accurate computation of the spectra is not the main goal of the present paper.

The final disc spectrum is computed by integration over the disc surface assuming an inclination angle equal zero

(i.e. top view). This integration procedure is an essential element of our model since the corona properties are radius-dependent: outer parts of the corona are predominantly responsible for the high energy extension of the spectrum and its hard X-ray slope while the inner, cooler parts of the corona mostly influence the soft X-ray range by producing moderately comptonized disc component.

All computations are done for a non-rotating black hole and the relativistic corrections are neglected.

3 CORONA PROPERTIES FOR CONSTANT δ

In this Section we show results obtained assuming a value of the advection parameter δ (Eq. 5) constant with radius.

3.1 The relative strength of the corona

The most important prediction of the model is a strong radial dependence of the strength of the corona. This dependence changes qualitatively with the accretion rate, mainly due to the presence of advection. Examples of radial dependences of the fraction of energy generated in the corona, $f(r)$, are shown in Figure 1 for a number of values of δ and \dot{m} .

Spatial extent of the corona is always finite, independently of \dot{m} and δ . The corona covers only an inner part of the disc from a certain outer radius R_{max} inwards.

At R_{max} all the energy is liberated in the corona for low accretion rates, if $\delta \neq 0$ (and for any \dot{m} when $\delta = 0$, i.e. if there is no advection). Consequently, at $r = R_{max}$ the accretion flow proceeds entirely through the corona. At larger radii no corona solutions of our equations exist since the Compton cooling provided by the disc is too large, under the adopted assumptions about the corona structure. There is therefore a strong and discontinuous change of accretion flow structure at R_{max} . For $r > R_{max}$ all the accretion proceeds through the disc whilst at $r = R_{max}$ the accretion proceeds through the corona, with the cold disc heated only by X-ray illumination. We envision that the change occurs through rapid heating and evaporation of the disc surface which takes place in order to maintain the thermal balance condition, but the detailed dynamics of this process is beyond the scope of our present model. Closer in, the relative strength of the corona decreases and, consequently, the relative fraction of the disc accretion increases.

The dependence of the radial extension of the corona, R_{max} , for $\delta = 0.75$ on the accretion rate is shown in Figure 2. The size of the corona is considerable, covering the disc up to $\sim 130R_{Schw}$ for accretion rate approaching $0.04 \dot{M}_{Edd}$, but R_{max} decreases significantly for smaller accretion rates, down to about $10R_{Schw}$ for sources radiating at 0.1 per cent of the Eddington luminosity. For accretion rates below $4 \times 10^{-4} \dot{M}_{Edd}$ the corona ceases to exist, as the Compton cooling is too strong while heating becomes inefficient. (see also Section 5.3).

Although the relative fraction of energy dissipated in the corona increases with radius (up to R_{max}) the actual energy flux decreases outwards. We can see that from the simple analytical solutions given in Appendix C of WCZ. Since f increases with the radius r approximately as $f \propto r^{3/8}$, the X-ray flux $F_X(r)$ decreases with radius: $F_X(r) \propto$

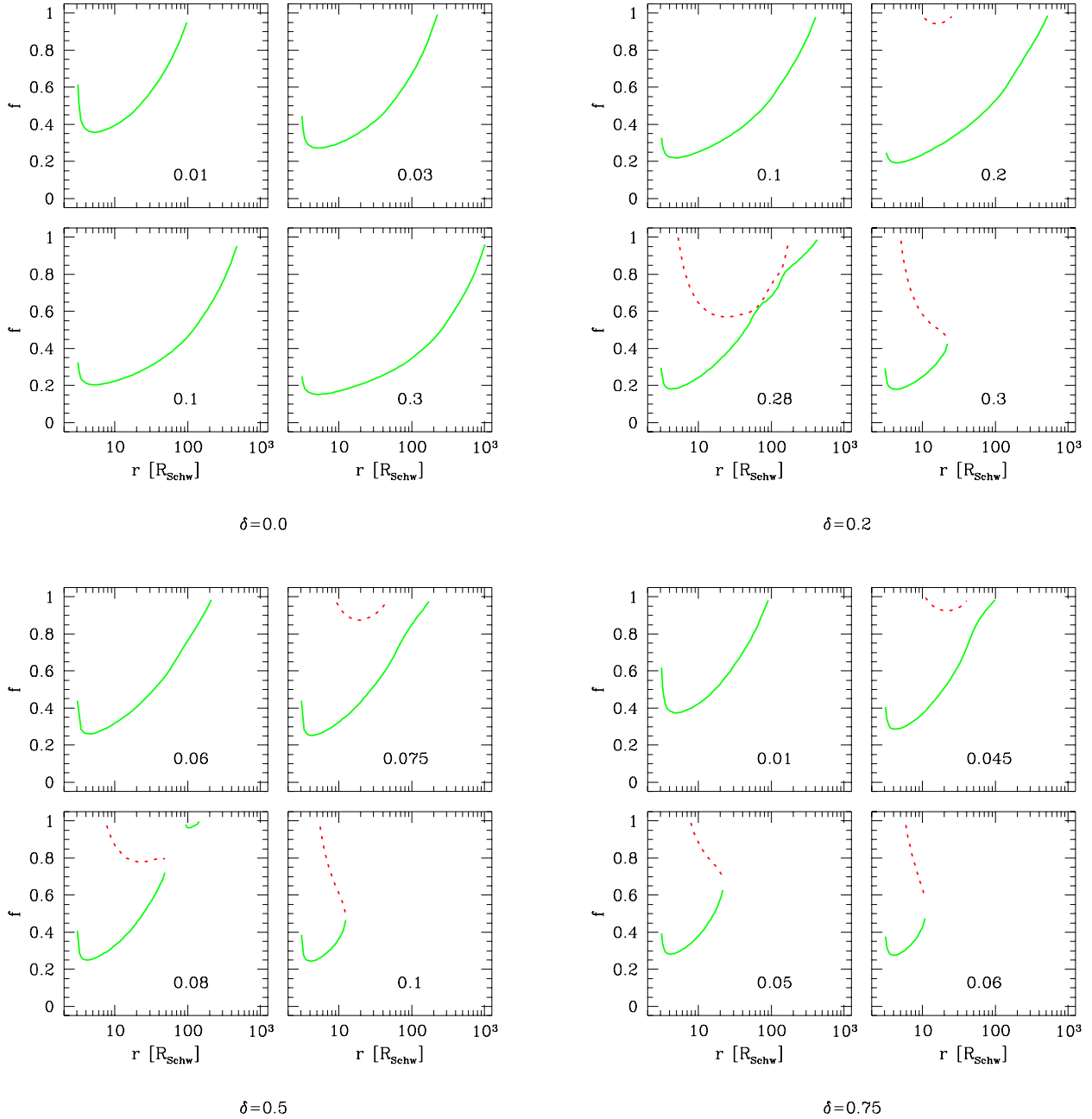


Figure 1. The fraction of the energy dissipated in the corona, f , as a function of radius for viscosity parameter $\alpha = 0.3$, mass of the black hole $10M_{\odot}$, and four values of the advection parameter δ (Equation 5): $\delta = 0, 0.2, 0.5$ and 0.75 . Labels inside panels refer to accretion rate.

$r^{-3+3/8}$. This may be important for detailed computations of relativistic smearing of the X-ray reprocessed component. However, we do not discuss this spectral component in the present paper.

A second branch of solutions appears when the accretion rate \dot{m} approaches a certain critical value, \dot{m}_{adv} . On this branch the cooling is dominated by advection and \dot{m}_{adv} is a function of δ : $\dot{m}_{\text{adv}} = 0.192, 0.069, 0.044$ for

$\delta = 0.2, 0.5, 0.75$, respectively (Figure 1). The exact topology of the two solutions is a rather complex function of δ and \dot{m} . For \dot{m} just above \dot{m}_{adv} the advective solution coexists with the radiative one in a range of radii. The two branches cross for somewhat higher \dot{m} and then separate, creating two spatial regions where both solutions can exist, with an intermediate range of r , where no solution is possible. The outer ring then shrinks rapidly as \dot{m} increases and disappears, the

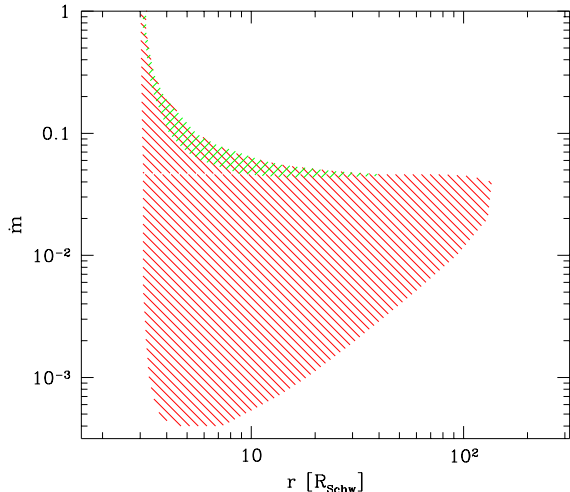


Figure 2. The dependence of the extension of the corona on the accretion rate for $\delta = 0.75$. Light shades mark the Compton cooling dominated solutions and the dark shades mark the region of both advection dominated and cooling dominated solutions. The viscosity parameter $\alpha = 0.3$ and the black hole mass is $10M_{\odot}$.

inner one does the same but more slowly. Mathematically, the solutions continue to (unphysical) $f > 1$ region creating closed loops.

For comparison we also plot in Figure 1 the radial dependence of the relative strength of corona obtained when the advection term was neglected ($\delta = 0$). Obviously, in this case only one branch of solutions appears. It is similar to the Compton-cooled branches of solutions with $\delta > 0$ for low accretion rates, $\dot{m} \lesssim 0.01$, i.e. the advection is then only a small correction to the energy balance. For larger \dot{m} the $\delta = 0$ solution is quite different from the advection-corrected solutions: the corona extends to much larger radii and no qualitative change with increasing \dot{m} is seen. It is clearly the advection term which is responsible for the complex topology of solutions seen in Figure 1.

The merging of the radiatively cooled solution with the advectively cooled solution has been previously found by Chen et al. (1995) and Björnsson et al. (1996) for an optically thin flow, not accompanied by any disc. Therefore, we also constructed an analogous $\log \dot{m} - \log \Sigma$ diagram for our coronal solution at $5R_{\text{Schw}}$ (Figure 3). We plot coronal surface density Σ_c versus the coronal accretion rate, $\dot{m}_c = \dot{m} f(r)$ where the value of factor $f(r)$ depends on the solution branch.

The two solution branches for a given total \dot{m} produce two points on this plot, since f is different on the two branches. The two solutions merge for $\dot{m} = 0.09$ (at our assumed radius $5R_{\text{Schw}}$, $\alpha = 0.3$ and $\delta = 0.75$), resulting in a continuous curve with both the fraction of energy carried by advection and the fraction of energy dissipated within the corona increasing with $f\dot{m}$. The uppermost point is characterized by $f = 1$, i.e. the whole energy is generated within the corona, but advection transports ≈ 90 per cent of the energy rather than 100 per cent. In our model the fully advective branch does not develop, due to the presence of the disc providing soft photons for Compton cooling. Mathematically, the fully-advective branch would ap-

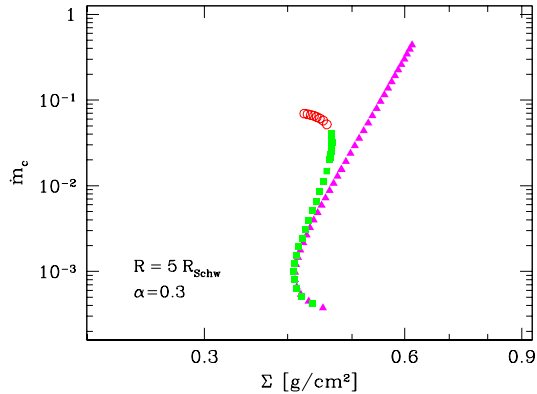


Figure 3. Coronal solutions shown in coronal accretion rate, \dot{m}_c , versus surface density in the corona, Σ , computed at $5R_{\text{Schw}}$ for $\alpha = 0.3$. Open circles show advection-dominated solution and solid squares show the Compton cooling dominated solution for $\delta = 0.75$. Note that the advective branch terminates when $F_{\text{adv}}/F_c = 0.9$, i.e. strongly advective solutions do *not* exist in our model. Solid triangles show the solution with $\delta(r)$ computed consistently through iterations (Section 4). Only one solution branch exists in this case, and it extends into fairly high \dot{m}_c (corresponding to total $\dot{M} \gg \dot{M}_{\text{Edd}}$). Black hole mass $M = 10M_{\odot}$.

pear for $F_{\text{soft}} = 0$, which would require unphysical condition $f = 1/[1 - \eta(1 - a)] > 1$. Thus the necessary presence of the soft photons from the disc suppresses in our model the fully advective branch, present in other optically thin solutions, e.g. ADAFs (see Section 5.1).

The existence of the advection dominated branch of solutions was not found by WCZ, and the reason for that is given in Section 3.2.2.

The viscosity parameter α has a strong influence on the existence and properties of the corona. For α lower than our assumed 0.3 the solutions are more limited in \dot{m} and radius, the more so the higher the advection coefficient δ . For example, for $\alpha = 0.03$ and $\delta = 0.2$ only very spatially limited solutions exist. For the same α but $\delta = 0.5$ no solutions exist.

3.2 Corona properties

3.2.1 Advection

In Figure 4 we show the ratio of the energy flux advected inwards with the coronal flow to the total dissipated flux for $\delta = 0.75$. For low accretion rates only the radiatively cooled solution exists and advection is not important. However, when \dot{m} approaches $\dot{m} = 0.1$, up to 40 per cent of the flux on this branch is carried by advection. This fraction depends on the radius.

For high accretion rates ($\dot{m} \gtrsim 0.04$) the second solution appears. This solution is cooled mostly by advection and it is similar to ADAF solutions. Since in that case most of the energy (more than 90 per cent) is liberated in the corona the accretion proceeds mostly through the corona itself.

3.2.2 Ion temperature and the geometry of the corona

The ion temperature decreases almost inversely with radius (see Figure 5 in WCZ and formulae in Appendix C in that paper). The pressure scale height of the corona, defined as

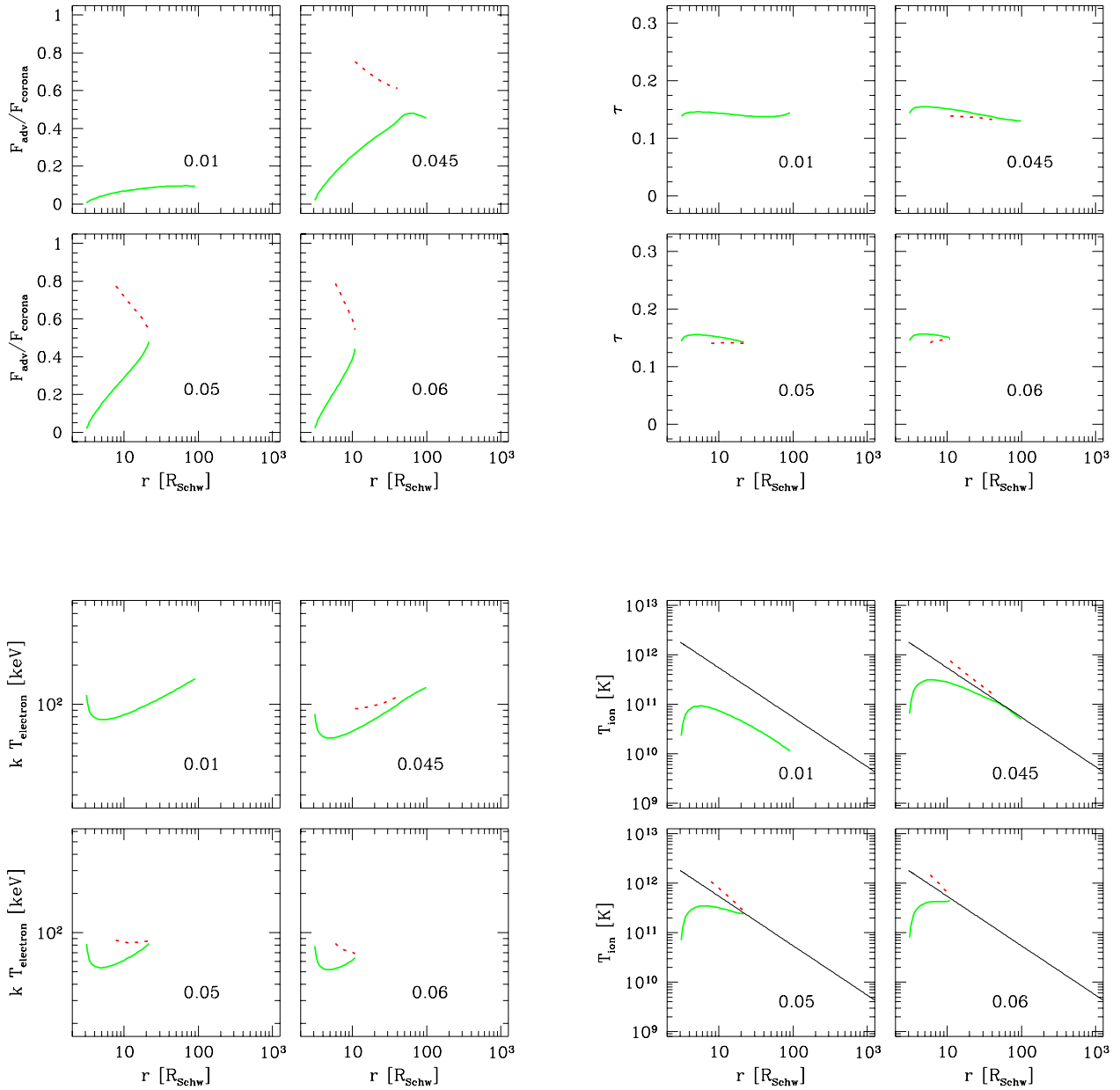


Figure 4. The radial dependencies of the ratio of the advected energy flux to the total flux generated in the corona (upper left panel), optical depth (upper right panel), electron temperature (lower left panel), and ion temperature (lower right panel), for viscosity parameter $\alpha = 0.3$, mass of the black hole $10M_{\odot}$, and $\delta = 0.75$. The thin straight line in the lower right panel shows the virial temperature. The dashed line shows advection-dominated solution whilst the solid line shows the solution cooled predominantly by Compton cooling. Labels inside panels refer to accretion rate.

$$H_P = \left(\frac{kT_i R^3}{GMm_H} \right)^{1/2} \quad (9)$$

increases almost linearly with radius and the ratio H_P/R is almost constant. The coronal accretion flow resembles actually a spherical accretion, similarly to the case of pure

ADAF flows. In such flows the ion temperature is of the order of the virial temperature and geometrical thickness of the flow is of the order of r . Sound velocity is close to the Keplerian velocity and is proportional to the radial velocity, where the proportionality coefficient is given by viscosity parameter α . However, our coronal solutions are generally

cooler and H_P/R ratio, although constant, is not equal 1. Nevertheless, the dependence of the radial velocity on radius is quite similar to the case of ADAF. In Figure 5 we plot the ratio of the radial to sound velocity, computed from the formula:

$$v_r = \frac{f\dot{M}}{4\pi R\Sigma_c}. \quad (10)$$

We see, that far from the marginally stable orbit v_r/v_s ratio is of order of α and is almost constant throughout the disc. The flow is then moderately subsonic, depending on the value of the viscosity parameter. Close to the marginally stable orbit our coronal flow, as well as ADAF solution, become transonic and continue as a free fall onto a black hole.

In this paper we use a simplified description of the vertical hydrostatic equilibrium and we have to check afterwards whether the solution can actually be in hydrostatic equilibrium. The approximate criterion is that the ion temperature should be smaller than the local virial temperature. We see from Figure 4 that T_i is usually lower than T_{vir} on the radiative branch, but $T_i > T_{\text{vir}}$ on the advective one. The same problem refers to the corona height as a function of radius. Since $H_P/R = \sqrt{T_i/T_{\text{vir}}}$, the ratio H_P/R can be larger than 1, i.e. the corona can be (very) geometrically thick. The reason for T_i exceeding T_{vir} can be seen from Equation 6: $T_i = (T_{\text{vir}}/\delta) \times (F_{\text{adv}}/F_c)$, i.e. T_i can approach and exceed T_{vir} if advection is dominant.

The super-virial ion temperature is the reason why advection-dominated solutions were not found by WCZ. In that paper the vertical structure was calculated much more carefully, assuming the hydrostatic equilibrium at the basis of the corona and allowing for the transonic vertical outflow from the corona. These solutions automatically prohibited the violation of the hydrostatic equilibrium at the basis of the corona. In that case the set of solutions for increasing accretion rates simply ended up as soon as the ion temperature reached the virial temperature (see Figure 2 of WCZ and Section 3.1 and 4.1 therein).

The same problem was noted by Narayan & Yi (1994) in the case of pure ADAF solutions and expressed as the problem of the Bernoulli constant being positive for ADAF. Therefore, the model with a hot medium being in hydrostatic equilibrium does not offer correct solution beyond certain value of accretion rate.

3.2.3 Electron temperature and the optical depth

Since the density in the corona decreases outwards the efficiency of Coulomb interaction between the ions and electrons decreases as well. However, both the disc and the corona bolometric luminosities go down rapidly with the radius. Therefore the electron temperature, T_e , rises outwards and the ratio of T_i/T_e decreases outwards. The highest value of T_e is of the order of 1.5×10^9 K, and it depends only weakly on \dot{m} and the viscosity parameter, α . Such a universal value is an interesting property of our model for lower accretion rates. At higher accretion rates, however, the outer radius of the corona contracts rapidly due to the advection and the maximum corona temperature also rapidly drops down with an increase of the accretion rate.

The optical depth of the corona is practically independent of radius, and very weakly dependent on other param-

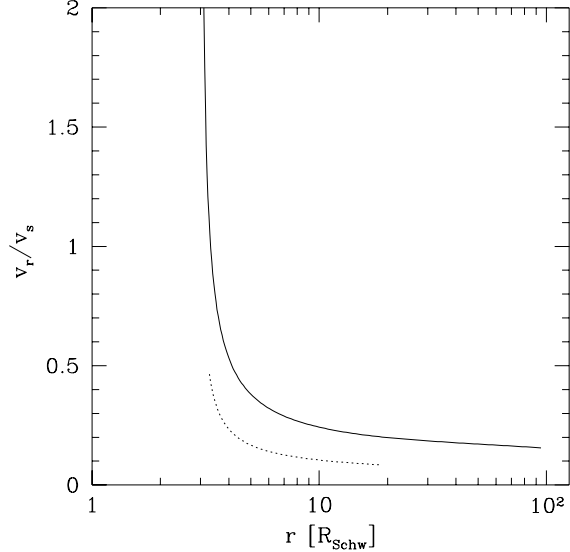


Figure 5. The ratio of the radial velocity to the sound velocity in the corona as a function of radius. The approximate constancy of v_r/v_s for $r \geq 10 R_{\text{Schw}}$ means that the geometry of the accretion resembles spherical accretion. The viscosity parameter $\alpha = 0.3$, mass of the black hole $10M_\odot$ and two values of the accretion rate \dot{m} : $\dot{m} = 0.01$ (continuous line) and $\dot{m} = 0.001$ (dashed line).

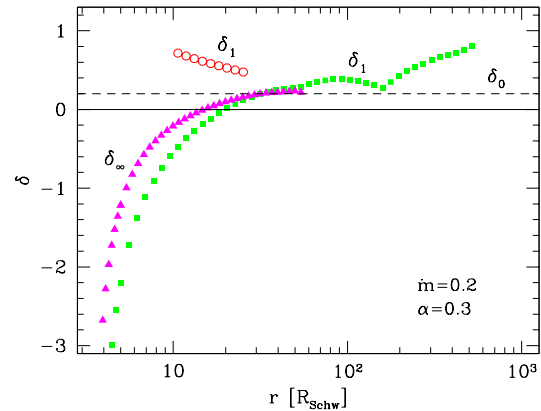


Figure 6. Coefficient $\delta(r)$ computed from the solution for $\dot{m} = 0.2$, and initial $\delta_0 = 0.2$ (equation 5). Solid squares represent the radiative branch, while the circles show the advective branch, after the first iteration (δ_1). On the advective branch the computed δ is systematically larger than the initial one which leads to the disappearance of this branch, when solution with consistent $\delta(r)$ is calculated. Solid triangles (δ_∞) show $\delta(r)$ for the converged solution, where only one branch remained.

eters; it is always between 0.1 and 0.2 (see Appendix C in WCZ).

4 SOLUTIONS WITH CONSISTENT $\delta(r)$

4.1 Corona structure

The assumption that the advection parameter δ is constant as a function of radius is not correct in general. As can

be seen from equation 5, δ is determined by radial derivatives of the ion temperature and pressure, hence it can be a function of radius. Since the topology of solutions depends rather sensitively on δ (Figure 1), we can expect significant changes of the topology if we consistently compute the $\delta(r)$ dependence.

As a first step, we show in Figure 6 the coefficient δ computed numerically from the solution obtained for initial constant $\delta_0 = 0.2$ and $\dot{m} = 0.2$ (labelled δ_1). For these parameters two solution branches exist: with radiative and advective cooling dominant (cf. Figure 1). On both branches the computed δ has a strong radial dependence. However, as Figure 1 shows again, the radiative branch is present for any δ , therefore we do not expect significant changes to its character, when solution with proper $\delta(r)$ is computed. The same is not true for the advective branch: the higher the δ , the narrower the range of this branch's existence in the $r-\dot{m}$ plane. Since the computed δ is now significantly larger than the initial one, we can expect a decrease of the importance of the advective branch.

Proper self-consistent solutions describing the flow can in principle be obtained either by solving radial differential equations containing explicitly the advection term expressed as derivatives given by equation 5, or by an iterative procedure correcting the distribution of $\delta(r)$ at each iteration step. First method was successfully applied by Chen, Abramowicz & Lasota (1997) and Narayan, Kato & Honma (1997) to obtain global solutions for ADAF flow. We used the second method, iterating solving the corona structure equations for a given $\delta(r)$ and computing the next approximation to $\delta(r)$. Our algorithm is very similar to the method used by Chen (1995): in order to find solution at a given radius r , we solve the equations at r and two auxiliary radii, $r - \Delta r$ and $r + \Delta r$ (assuming $\delta(r \pm \Delta r) = \delta(r)$, but the solution is insensitive to this particular condition). We then compute the corrected δ from equation 5 and compute the corrected structure. When convergence is achieved, we proceed to the next radius.

Iterating the solution for the advection-dominated branch quickly leads to its disappearance. The radiative branch shrinks somewhat (R_{\max} decreases), especially for \dot{m} such that the advected fraction close to R_{\max} was substantial in the non-iterated solution. In other words, only the solutions with rather low advective cooling survive.

Figure 6 (points labelled δ_∞) shows an example of the iterated $\delta(r)$ dependence. The iterated $\delta(r)$ is positive for larger radii, where advection is a cooling process, but it changes sign for smaller radii, as advection becomes a locally heating process. The same trend was obtained for optically thick discs calculated taking into account advection, departure from the Keplerian rotation and the transonic character of the flow close to the marginally stable orbit (Muchotrzeb & Paczyński 1982; Abramowicz et al. 1988). The heating role of advection increases dramatically close to the marginally stable orbit since the energy dissipation there approaches zero.

In Figure 7 we show examples of the converged solutions of the corona structure as functions of \dot{m} and α . The corona is strongest at its outer edge, although f is not always 1 at $r = R_{\max}$. Similarly to solutions with constant δ , the electron temperature is ~ 100 keV while the optical thickness is ~ 0.15 . Advection is never important as a cooling process. At small radii, $r \lesssim 20 R_{\text{Schw}}$, δ changes sign,

so the advective flux contributes to heating. In this region the solution exist for $\dot{m} \gtrsim 4 \times 10^{-4}$, and up to $\dot{m}_c \sim 1$, i.e. the Eddington luminosity in the corona. The topology of solutions represented on the $\dot{m}-\Sigma$ diagram change as well (Figure 3): the solution forms a single branch only.

The solutions are sensitive to the value of the viscosity parameter α . For low α the solutions are generally rather limited spatially. Moreover, for $\alpha \leq 0.1$ the ion temperature strongly exceeds the virial temperature, so the solutions can hardly be considered physically acceptable.

The value of the mass of the central black hole influences the results only very slightly. Solutions for $M = 10^8 M_\odot$ practically overlap those for $M = 10 M_\odot$. This is to be expected (see e.g. Björnsson & Svensson 1992 and references therein), since the only dependence on the central mass in our model is through the temperature of the soft flux, which can affect the Compton amplification factor, but the dependence $A(T_0)$ is very weak for steep (soft) spectra.

4.2 Radiation spectra

Spectra predicted by the model are rather soft and dominated by the disc emission. Examples are plotted in Figure 8 for parameters characteristic for AGN and GBH. Generally, the power law components are harder for lower \dot{m} .

For accretion rates of order of $0.05 \dot{M}_{\text{Edd}}$, typically expected in Seyfert galaxies, the amount of hard X-ray emission predicted by the model is negligible and the high energy index far too steep, so the present model does not offer a promising description. On the other hand, the original model of WCZ (with neglected advection) reproduced well the typical properties of AGN (see Czerny et al. 1997 for radio quiet quasars and Seyfert galaxies, and Kuraszewicz et al. 1999 for NLS1 galaxies; see also the corona parameters determined for MCG+8-11-11 by Grandi et al. 1998).

For the Galactic black holes the general trends are similar to those for AGN. For very low accretion rates ($\dot{m} \lesssim 0.01$) the model predicts considerable hard X-ray emission from the corona, although the spectra are somewhat steeper than those resulting from the original model by WCZ (Janiuk & Czerny 1999). Very steep spectra are predicted for $\dot{m} \gtrsim 0.1$, i.e. corresponding to the high or very high state of stellar black hole systems, while $\Gamma \sim 2$ in the observed spectra of e.g. soft X-ray transients (Życki, Done & Smith 1998).

5 DISCUSSION

In this paper we considered the accreting corona model. Main features of the model and differences from other hot accretion flow solutions are, firstly, the presence of a cool, optically thick disc supplying soft photons for Comptonization in the corona, and secondly, the condition for (vertical) stratification of the flow into the two phases due to thermal instability. Since in this model the accreting coronal plasma is hot, optically thin and geometrically thick, it is necessary to include the radial energy transport (advection), similarly to the optically thin ADAF solutions and optically thick, slim discs.

The structure of solutions crucially depends on whether the advective flux is solved for consistently – i.e. the coefficient δ (Eq. 5) is a function of radius – or $\delta(r)$ is assumed

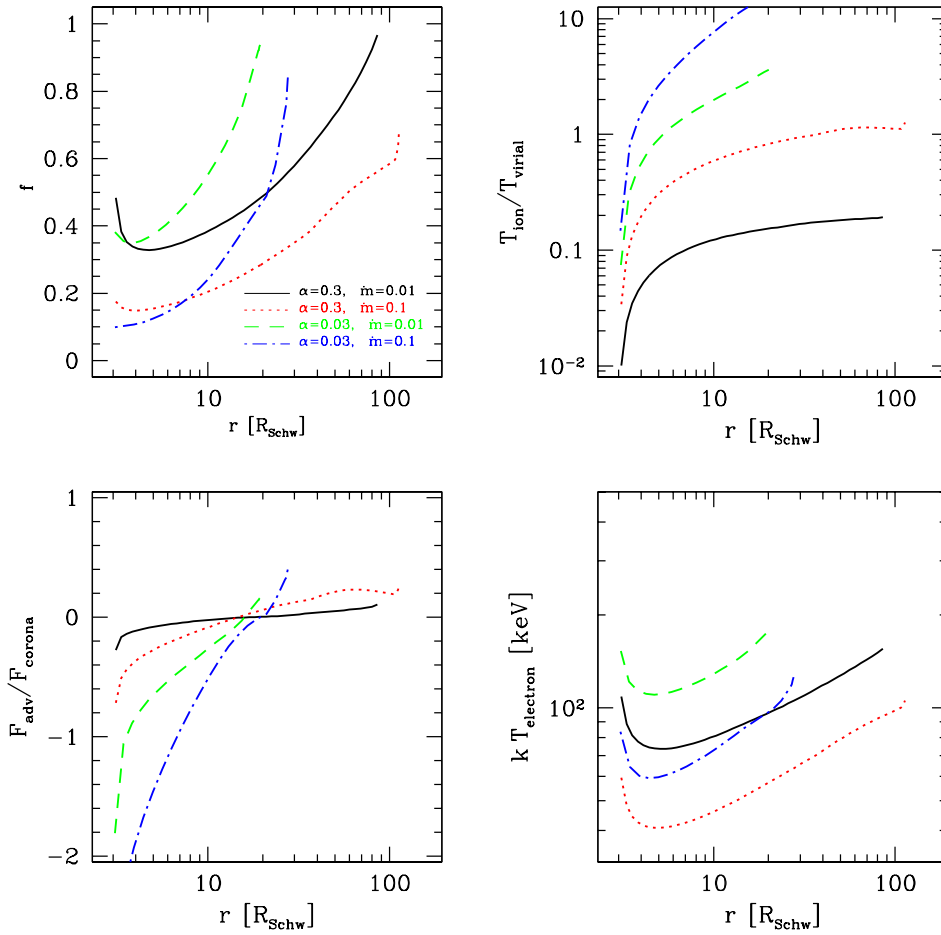


Figure 7. Examples of the corona structure computed with consistent solution for the advection coefficient $\delta(r)$. Two values of the viscosity coefficient α are shown, with two values of \dot{m} for each α , as labelled. The solutions were computed for $10 M_{\odot}$, but the dependence on the BH mass is negligible.

constant, although there are certain properties of the solutions independent of the δ -prescription.

For a constant δ , at a given radius (smaller than a certain maximum value) there is either one solution – radiatively cooled through Compton process – or two solutions, one radiatively cooled and the other advection-dominated. For radii larger than the maximum one no coronal solutions exist. Whenever two solutions are possible, there is always a critical value of the accretion rate for which the two solutions merge and no solutions are found for higher accretion rates.

Similar effect is seen when studying the radial structure of coronal solutions. At very low accretion rates (below $\dot{m} \sim 4 \times 10^{-4}$) there are no coronal solutions. At larger \dot{m} the radiatively cooled solution appears, which covers an inner part of the disc. This solution was previously found by WCZ. The fraction of the disc covered by the corona increases with the accretion rate but the fraction of radiation emitted by the corona decreases. At even higher \dot{m} (above $\dot{m} \approx 0.04$, depending on δ) a second, advection-dominated solution emerges, if the corona structure equations allow for the ion temperature to be higher than the virial temperature. The two solutions merge at the outer edge of the

corona. With further increase of the accretion rate, the region covered by the corona contracts rapidly, with no corona present for $\dot{m} \gtrsim 0.1$ (for the viscosity parameter $\alpha = 0.3$). Smaller α leads to solution merger for even lower accretion rates, as found previously by e.g. Abramowicz et al. (1995) and Björnsson et al. (1996).

The existence of the advection-dominated solutions was automatically excluded in the original formulation of the model by WCZ – instead, they simply observed the disappearance of the single, radiation cooled solution with an increase of the accretion rate due to the ion temperature reaching the virial value.

When the $\delta(r)$ function is solved for, we obtain only one solution branch. It is cooled by radiation i.e. with advective cooling negligible. In fact, advection changes sign for $r \leq 20 R_{\text{Schw}}$ i.e. it acts as a heating process. The properties of this branch are similar to those of the radiatively cooled branch obtained for a constant δ : the solution exist for $\dot{m} > 4 \times 10^{-4}$, and the corona is strongest at its outer edge. For radii such that advection is a heating process there, this solution can exist up to rather high \dot{m} , even formally exceeding \dot{M}_{Edd} in the corona. It disappears only when the temperature of the disc flux reaches the (decreas-

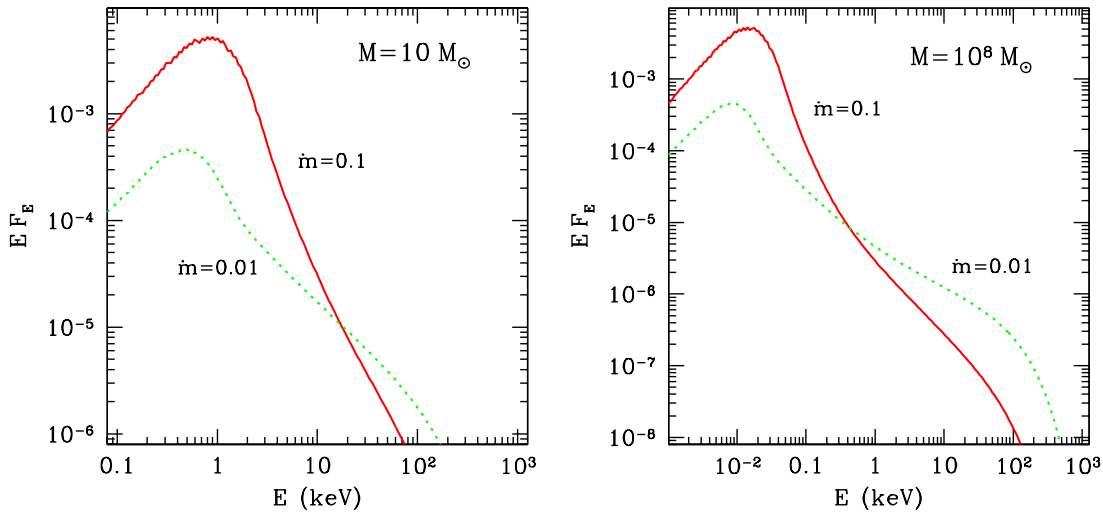


Figure 8. The radiation spectra for $M = 10 M_{\odot}$ (left panel) and $M = 10^8 M_{\odot}$ (right panel). Two values of the accretion rate are plotted, as labelled, and the viscosity parameter $\alpha = 0.3$. Corresponding solutions of the corona structure are plotted in Figure 7.

ing) electron temperature in the corona, but it is strongly super-virial already for lower \dot{m} .

5.1 Comparison with other hot, optically thin solutions

Our solutions show general similarity to other hot, optically thin disc solutions (SLE; Abramowicz et al. 1995; Chen et al. 1995; Björnsson et al. 1996; Narayan & Yi 1995; Zdziarski 1998; see Kato et al. 1998 for general discussion). There are also, however, certain important differences, as a direct consequence of the assumptions specific to our model.

When plotted on the \dot{m} - Σ diagram (Figure 3), our solutions for constant δ form two branches, merging for certain maximum \dot{m} . Both the existence of the two branches and their merging was found previously. However, as opposed to ‘conventional’ ADAF solutions, strongly advection-dominated branch does not appear in our model, due to substantial Compton cooling. For the same reason our solutions disappear for lower viscosity, $\alpha \leq 0.03$, while no such effect is observed in the above mentioned solutions, where the adopted cooling mechanism can usually be made sufficiently inefficient (see below).

We obtain an increase of the maximum allowed coronal \dot{m} , when we solve for the advective flux (i.e. $\delta(r)$). This has also been found previously by Chen (1995). Again, however, the advection-dominated branch does not appear in our solution, and the solution disappears for low viscosity. None of these effects has appeared in the Chen (1995) work.

Hot discs cooled by comptonization of external soft photons were considered by Zdziarski (1998), as a generalization of the SLE solution. However, the source of soft photons was not specified in that work i.e. the soft flux could implicitly be assumed to be small, if required. Therefore the general properties of the solutions found were in close agree-

ment with the previous solutions where bremsstrahlung was usually assumed as the radiative cooling process. For example, the strongly advective branch is present in Zdziarski (1998) solution, in spite of the efficient radiative cooling. The Compton parameter $y \equiv 4kT_e/m_e c^2 \tau$ is ~ 1 in that work (it is ~ 0.1 in our solutions), which indeed requires very low F_{soft} in order not to suppress the advectively-cooled branch.

Where an ADAF-like disc is assumed to co-exist with a cold, optically thick disc (e.g. Esin et al. 1997), the transition radius is an adjustable parameter. In our work the additional equation (Eq. 1) resulting from the thermal instability condition closes the structure equations, thus enabling us to compute the transition radius.

5.2 Super-virial ion temperature

The ion temperature in an optically thin ADAF flow tends to be larger than the local virial temperature and the Bernoulli constant for such a flow is positive. Therefore such solutions are not possible without some kind of outflow (e.g. Narayan et al. 1997, Blandford & Begelman 1999).

The same problem affects the advection dominated branch of our coronal solutions and the iterated solutions obtained for low α . Such a corona violates the assumption of the hydrostatic equilibrium. Coronal gas with ion temperature exceeding the local virial temperature cannot flow in, as assumed in our model or ADAF solutions. If strong outflow indeed developed, no accretion would take place, switching off the energy source. A moderate transonic outflow from the corona surface perpendicular to the disc does not provide a solution. It was already included in the original formulation of the model by WCZ and it did not prevent the disappearance of coronal solutions for accretion rates higher than $\dot{m} \sim 0.1$. A magnetic wind can provide a solution, provided that the outflow launched at certain radius carries

away *more* angular momentum than what is locally necessary for accretion to proceed (Blandford & Begelman 1999). However, at this stage such solutions are rather arbitrary.

5.3 Corona formation at its outer edge

Our model does not provide a mechanism for disc evaporation. Instead, it allows to check whether the corona, if formed, can exist in hydrostatic and thermal equilibrium. The outer edge of our corona is therefore the maximum radius at which those conditions are satisfied. Since we did not consider two-dimensional flow, our transition from a bare disc to a coronal solution is sharp. The transition would become smooth if the radial conduction were included (e.g. Honma 1996), but this would require two-dimensional computations, since the radial thickness of the transition zone is expected to be same as the vertical thickness (see discussion by Dullemond 1999). The coexistence of the bare disc and the disc/corona at R_{\max} does not contradict the analysis of Dullemond & Turolla (1999) since the coronal part is not strongly advection-dominated, with approximately half of the energy (or less) carried by advection and the remaining energy radiated away locally, as in SLE.

The mechanism leading to corona formation is still unspecified. It may be related either to disc instabilities, or magnetic phenomena. The coronal solutions are generally within the standard disc radiation pressure instability zone (e.g. Janiuk & Czerny 1999), but this does not seem a strong argument in favour of the first possibility.

The transition radius, R_{\max} , in our models is generally rather smaller than the outer radius of the ADAF flow in typical applications, which is assumed $\sim 10^4 R_{\text{Schw}}$ (e.g. Esin et al. 1997). Since our description of the flow applies in principle to the outer part of an ADAF solution, where the hot flow and the cold disc flow are assumed to overlap (Esin et al. 1997), it may mean that large ADAF radii would also be difficult to achieve if the disc/corona coupling was correctly included. However, our result should be rather treated as an indication of a possible problem and not a definite answer. The model depends rather sensitively on the adopted description of the disc/corona coupling, expressed through Equation 2, as was shown for a non-advective corona by Janiuk & Czerny 2000. The simple change from the bremsstrahlung contribution from 2/3 (our assumption) to 3/7 (Krolik 1998) would only change the results quantitatively by radially expanding the region of coronal solutions but lowering the optical depth of the corona. However, better description of the transition region with disc evaporation included may change the results more significantly. It may also provide an explanation of the formation of ADAF part. Unfortunately, although some preliminary, partial results are available (e.g. Meyer & Meyer-Hofmeister 1994, Dullemond 1999, Różańska & Czerny 1999), they are still not directly applicable to the models and further research is needed. It may also be true that the radial extension of the overlapping region will appear to be small, as suggested by Dullemond (1999), thus further complicating the prediction of location of the disc/ADAF transition.

6 CONCLUSIONS

- Advection-dominated branch of coronal solutions does not represent a physically acceptable description of the flow.
- Accreting corona solutions are predominantly Compton-cooled and, for small radii, exist for all accretion rates larger than $\approx 4 \times 10^{-4} \dot{M}_{\text{Edd}}$.
- Spectral slopes predicted by accreting corona models for AGN and GBH are too steep in comparison with observations so the disruption of the innermost part of the disc or magnetically driven outflow seem to be required.

ACKNOWLEDGEMENTS

This work was supported in part by grant 2P03D01816 of the Polish State Committee for Scientific Research.

REFERENCES

- Abramowicz M.A., Czerny B., Lasota J.P., Szuszkiewicz E., 1988, ApJ, 332, 646
- Abramowicz M.A., Chen X., Kato S., Lasota J.P., Regev O., 1995, ApJL, 438, L37
- Begelman M.C., McKee C.F., Shields G.A., 1983, ApJ, 271, 70
- Bisnovatyi-Kogan G.S., Blinnikov S.I., 1977, A&A, 59,111
- Björnsson G., Svensson R., 1992, ApJ, 394, 500
- Björnsson G., Abramowicz M.A., Chen X., Lasota J.-P., 1996, ApJ, 467, 99
- Blandford R.D., Begelman M.C., 1999, MNRAS, 303, L1
- Chen X., Abramowicz M.A., Lasota J.-P., Narayan R., Yi I., 1995, ApJ, 44, L61
- Chen X., 1995, MNRAS, 275, 641
- Chen X., Abramowicz M.A., Lasota J.-P., 1997, ApJ, 476, 61
- Collin-Souffrin S., Czerny B., Dumont A.-M., Życki P.T., 1996, A&A, 314, 393
- Czerny B., Dumont A.-M., 1998, A&A, 338, 386
- Czerny B., Witt H.J., Życki P.T., 1996, Acta Astr. 46, 9,
- Czerny B., Witt H.J. Życki P.T. 1997, in *ESA SP-382*, 2nd INTE-GRAL Workshop, “The Transparent Universe”, eds. C. Winkler, T. Courvoisier and Ph. Durouchoux, p. 397
- Czerny B., Zbyszewska M., 1991, MNRAS, 249, 634
- Dullemond C.P., 1999, A&A, 341, 936
- Dullemond C.P., Turolla R., 1999, ApJ, 503, 361
- Esin A.A., McClintock J.E., Narayan R., 1997, ApJ, 489, 865
- Górecki A., Wilczewski W., 1984, Acta Astr., 34, 141
- Grandi P., Haardt F., Ghisellini G., Grove E.J., Maraschi L., Urry C.M., 1998, ApJ, 498, 220
- Haardt F., Maraschi L., 1991, ApJ, 380, L51
- Haardt F., Maraschi L., Ghisellini G., 1997, ApJ, 476, 620
- Honma F., 1996, PASJ, 48, 77
- Ichimaru S., 1977, ApJ, 214, 840
- Janiuk A., Czerny B., 2000, *New Astronomy* (in press)
- Kato S., Fukue J., Mineshige S., 1998, *Black Hole Accretion Disks*, Kyoto University Press, Kyoto
- Krolik J.H., 1998, ApJ, 498, L13
- Krolik J.H., McKee C.F., Tarter C.B., 1981, ApJ, 249, 422
- Kuraszkiewicz J., Wilkes B., Czerny B., Mathur S., 1999, ApJ, in press
- Liang E.P.T., Price R.H., 1977, ApJ, 218, 247
- Madejski G. M., 1999, in Abramowicz M., Björnsson G. & Pringle J., Eds., “Theory of Black Hole Accretion Disks”, Cambridge University Press, 21

- Meyer F., Meyer-Hofmeister E., 1994, *A&A*, 288, 175
Muchotrzeb B., Paczyński B., 1982, *Acta Astr.* 32, 1
Mushotzky R.F., Done C., Pounds K.A., 1993, *ARA&A*, 31, 717
Narayan R., Yi I., 1994, *ApJ*, 428, L13
Narayan R., Yi I., 1995, *ApJ*, 452, 710
Narayan R., Kato S., Honma F., 1997, *ApJ*, 476, 49
Poutanen J., Svensson R., 1996, *ApJ*, 470, 249
Pozdnyakov L.A., Sobol I.M., Sunyaev R.A., 1983, *Ap. Space Phys. Rev.*, 2, 189
Różańska A., Czerny B., Życki P.T., Pojmański G., 1999, *MNRAS*, 305, 481
Różańska A., Czerny B., 1999, *MNRAS* (submitted)
Shakura N.I., Sunyaev R.A., 1973, *A&A*, 24 337
Shapiro S.L., Lightman A.P., Eardley D.M., 1976, *ApJ*, 204, 187 (SLE)
Tanaka Y., Lewin W.H.G., 1995, in Lewin W.H.G., van Paradijs J., van den Heuvel E.P.J. eds., *Cambridge Astrophys. Ser. Vol. 26, "X-ray binaries"*, Cambridge Univ. Press, Cambridge, p. 126
Torricelli-Ciamponi G., Courvoisier T.J.-L., 1998, *A&A*, 335, 881
Witt H.J., Czerny B., Życki P.T., 1997, *MNRAS*, 286, 848 (WCZ)
Zdziarski A.A., 1998, *MNRAS*, 296, L51
Życki P.T., Collin-Souffrin S., Czerny B., 1995, *MNRAS*, 277, 70.
Życki P. T., Done C., Smith D. A., 1998, *ApJ*, 496, L25

This paper has been processed by the authors using the Blackwell Scientific Publications L^AT_EX style file.